



Lithologic Hydrocarbon Accumulations in the Upper Jurassic Kalazha Formation in the Foreland Slope, the South Marginal Junggar Basin, Northwest China

Gang Liu^{1*}, Xue-Feng Qi¹, Jian-Zhong Li¹, Ming Zhu², Bo Yuan² and Zhi-Chao Pang²

¹Research Institute of Petroleum Exploration and Development, China National Petroleum Corporation, Beijing, China, ²Research Institute of Petroleum Exploration and Development, Xinjiang Oilfield, China National Petroleum Corporation, Karamay, China

OPEN ACCESS

Edited by:

Wenjing Lin,
Institute of Hydrogeology and
Environmental Geology (CAGS), China

Reviewed by:

Binfeng Cao,
Institute of Geology and Geophysics
(CAS), China
Changyu Fan,
Northwest University, China

*Correspondence:

Gang Liu
584670774@qq.com

Specialty section:

This article was submitted to
Solid Earth Geophysics,
a section of the journal
Frontiers in Earth Science

Received: 17 November 2021

Accepted: 17 January 2022

Published: 25 February 2022

Citation:

Liu G, Qi X-F, Li J-Z, Zhu M,
Yuan B and Pang Z-C (2022) Lithologic
Hydrocarbon Accumulations in the
Upper Jurassic Kalazha Formation in
the Foreland Slope, the South Marginal
Junggar Basin, Northwest China.
Front. Earth Sci. 10:816960.
doi: 10.3389/feart.2022.816960

The foreland slope in the south marginal Junggar Basin (SMJB) is geologically favorable for mass lithologic oil and gas reservoir accumulation. Based on outcrops, thin sections, individual-well facies, and cross-well stratigraphic correlation, the stratigraphic distribution and features of the Upper Jurassic Kalazha Formation were investigated in the SMJB. There are two sedimentary sources in the southwest and southeast Kalazha Formation, which thin out from south to north and vanish in the northern slope. Fan deltas occur in the southwest, and braided river deltas occur in the southeast. Kalazha reservoir rocks and sedimentary facies were predicted using joint 2D and 3D seismic impedance inversion. According to the overall analysis, the Kalazha Formation in the foreland slope is favorable for hydrocarbon accumulation, considering structural highs as the destination of long-term hydrocarbon migration and the updip wedge-out zone in the north with potential lithologic traps. The accumulation model was established with source rocks, reservoir rocks, caprocks, and migration systems for the lithologic hydrocarbon reservoirs in the Kalazha Formation in the SMJB. As per the model and regional stratigraphic and structural features, Kalazha lithologic hydrocarbon reservoirs mainly formed in the annular updip wedge-out zone in the foreland slope. Our deliverables may provide useful information for mass lithologic hydrocarbon accumulation in the foreland slope and deep to ultra-deep hydrocarbon exploration in the SMJB.

Keywords: Kalazha Formation, lithologic hydrocarbon reservoir, foreland slope, south marginal Junggar Basin, accumulation condition, accumulation model

INTRODUCTION

Lithologic reservoirs, especially large and extremely large lithologic oil and gas fields (provinces), are important to hydrocarbon exploration and reserves and production increases, the proved reserves of which account for 80% of the total reserves (Yuan et al., 2003; Jia et al., 2007; Tao et al., 2017). There are fewer and fewer structural reservoirs, which are less challenging for exploration, and hydrocarbon exploration is now focusing more on elusive lithologic reservoirs (Fu et al., 2020; Liang and Li, 2020).

The slope zone in a foreland basin is among the primary areas deposited with clastic lithologic reservoirs. According to the theory of structure-sequence-dominated hydrocarbon accumulations in

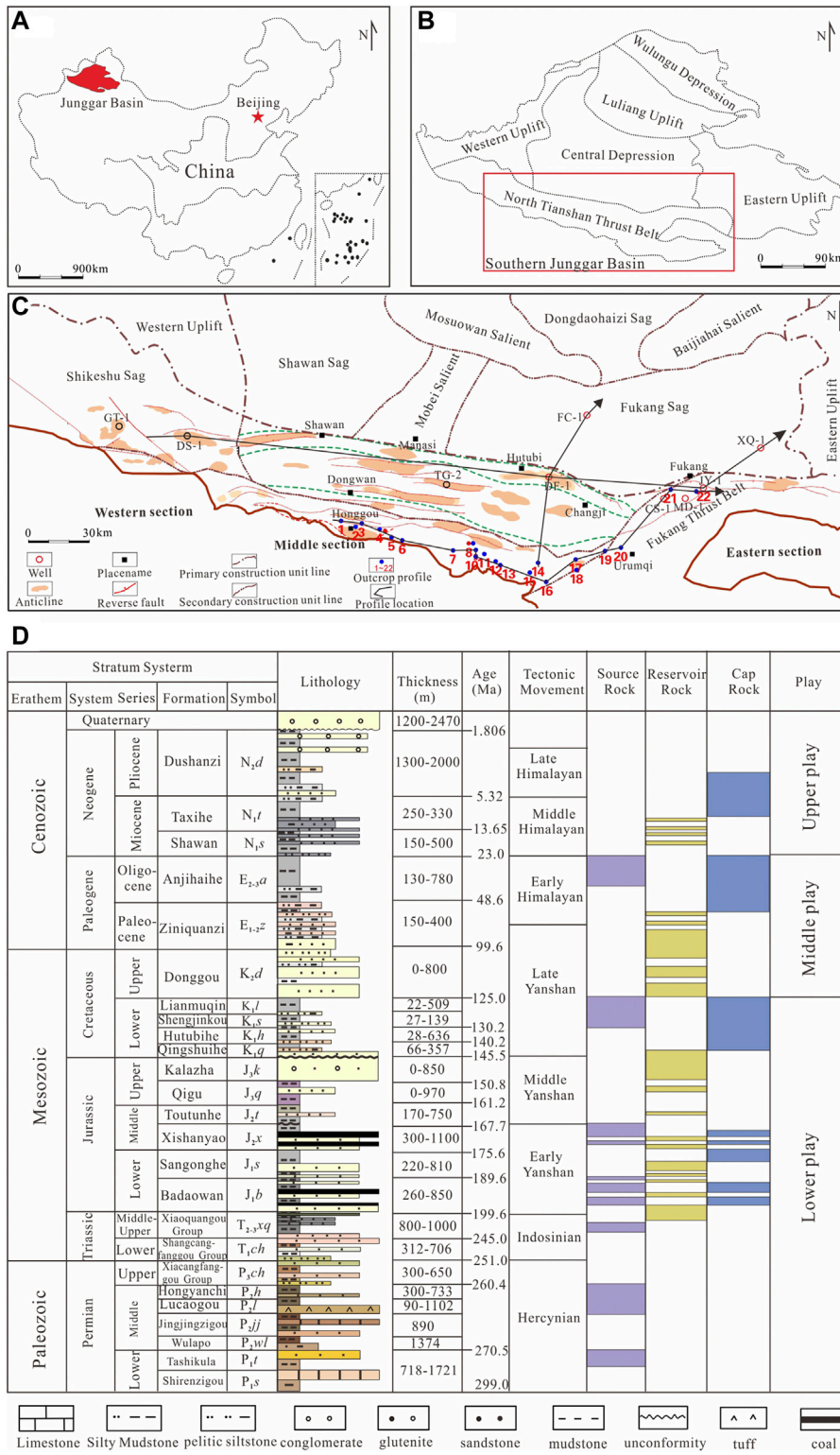


FIGURE 1 | (A) Regional location of the Junggar Basin in northwest China. **(B)** Tectonic units and the south marginal Junggar Basin (SMJB). **(C)** Location of the subunits, typical wells, and cross-sections. **(D)** Composite stratigraphic column in the MSTB.

a continental foreland basin, the occurrence of lithologic traps is dominated by six boundaries, such as lithologic pinch-out boundary, and four surfaces, such as fault surface. The distribution of lithologic reservoirs is dominated by three surfaces (maximum flooding, unconformity, and fault surfaces). Mass lithologic-stratigraphic hydrocarbon accumulation is related to the fans in the thrust belt, deltaic plains, and fronts in the slope zone in a continental foreland basin (Jia et al., 2008; Tao et al., 2017). Based on a portfolio of proven techniques for the exploration and evaluation of lithologic-stratigraphic reservoirs, elusive lithologic reservoir exploration in the thrust belt could be effectively performed in the slope zone, in addition to the structural belt. Recent hydrocarbon exploration has focused more on deep to ultra-deep zones. Moreover, large deep-seated structures and clastic lithologic reservoirs in the slope zones in foreland basins will become important targets for large-scale reserves increases. Most foreland basins in China are multicyclic superimposed basins with multi-phase tectonic movements and complicated hydrocarbon accumulation. Limited by deep to ultra-deep data, it is challenging to pinpoint lithologic reservoirs in deep to ultra-deep slope zones in foreland basins.

The south marginal Junggar Basin (SMJB) (**Figure 1**) is rich in hydrocarbon resources (Zhen et al., 2019), where large hydrocarbon reservoirs may occur. Exploration activities in the SMJB began in 1936 and have targeted shallow zones, including the Paleogene and Cretaceous Systems before 2008, where some small gas-rich fields were discovered. Since 2008, exploration has turned to deep-seated large structural traps in and below the Cretaceous System. Successes in Well GT1 at the beginning of 2019 (Du et al., 2019) indicated substantial exploration potential in the SMJB. Given the large area and promising accumulation conditions, large lithologic reservoirs may continuously occur in the slope zone in the foreland basin; thus, the slope zone may become an important reserves successor (Zhang and Liu, 2002).

We focused on the sedimentation, reservoirs, and hydrocarbon accumulation in the Jurassic Kalazha Formation in the SMJB; a model of lithologic hydrocarbon accumulation was established in the slope zone of the foreland basin and predicted promising areas rich in lithologic reservoirs. Research findings may provide useful information for hydrocarbon exploration in this region.

GEOLOGIC SETTING

The SMJB went through multi-phase tectonic-sedimentary evolution after the Permian Period, including foreland basin evolution from the Permian Period to Triassic Period, fault subsidence and compresso-shear in the Jurassic Period, intracontinental depression evolution from the Cretaceous Period to Paleogene Period, and rejuvenated foreland basin evolution from the Neogene Period to Quaternary Period (Wu et al., 2002; Wu et al., 2005; Wan et al., 2005; He et al., 2018). Foreland basin evolution may also occur in the late Jurassic Period as per the Qigu anticline and intense denudation in the Middle and Upper Jurassic Series (Kuang and Qi, 2006). Due to

multi-phase tectonic-sedimentary processes in the SMJB, the slope zone in the thrust belt was geologically favorable for mass lithologic hydrocarbon accumulation (Zhang and Liu, 2002; Liu et al., 2019).

The SMJB has several packages of Permian-Paleogene source rocks (**Figure 1D**) (Tian et al., 2017; Wei et al., 2010) and major source rocks, including dark mudstones, carbonaceous mudstones, and coals, occurring in the Jurassic Badaowan (J_{1b}), San'gonghe (J_{1s}), and Xishanyao (J_{2x}) Formations (Qiu et al., 2008; Chen et al., 2017; Chen et al., 2019). The source center extends widely in the Fukang sag, Shawan sag, piedmont thrust belt, and Sikeshu sag (Wei et al., 2007; Wang et al., 2013; Chen et al., 2015). Source rocks, 600–800 m thick, are mature to post mature.

Several packages of effective reservoir rocks are developed in the deep Cretaceous Qingshuihe Formation and Jurassic Kalazha and Toutunhe Formations in the SMJB (Lei et al., 2012; Tian et al., 2017). Stable basal sandy conglomerates in the Qingshuihe Formation are laterally connected, favorable for lateral hydrocarbon migration (Liu et al., 2018). Kalazha reservoir rocks are mainly thick, blocky sandy conglomerates and sandstones of hundreds of meters thick with the sedimentary source in the south (Schneider et al., 1992; Shan et al., 2014; Gao et al., 2020).

The upper, middle, and lower reservoir-seal assemblages are separated by the regional mudstones in the Taxihe Formation (N_{1t}), Anjihaihe Formation (E_{2-3a}), and Tugulu Group (K_{1tg}) in the SMJB (Li et al., 2003; Li et al., 2006). Oil and gas are mainly concentrated in the middle assemblage (Xiao et al., 2011; Kuang et al., 2012). The Kalazha Formation, with promising accumulation conditions for hydrocarbon preservation, is covered with 500–1,000-m-thick Tugulu mudstones in the lower assemblage. The overpressure in the Tugulu Group, with a pressure coefficient above 1.8, will further enhance the sealing performance of mudstones (Tigert and Al-Shaieb, 1990; Magara, 1993; Darby et al., 1996). In addition to structural reservoirs in the Qingshuihe Formation, large lithologic reservoirs may be found in the Kalazha Formation.

STRATIGRAPHIC DISTRIBUTION

Well data are insufficient for the study of stratigraphic distribution because only a limited number of wells were drilled into the Kalazha Formation. Thus, we made full use of piedmont outcrop, well, and 2D and 3D seismic data to investigate stratigraphic distribution in the Kalazha Formation. Due to the influence of compressional tectonic movements in the Middle and Late Jurassic Epochs, the Kalazha Formation has been intensely denuded and is limited within Hutubi, Fukang, and some piedmont areas in the middle and eastern parts of the SMJB.

In the area of interest, the Kalazha Formation was drilled by some exploratory wells, i.e., DF-1, JY-1, JY-2, CS-1, and MD-1. Well DF-1 did not penetrate the Kalazha Formation. As per log data, the Kalazha Formation consists of gray and brown conglomerates, sandy conglomerates, and medium-to-fine-grained sandstones sandwiched with thin siltstones and pelitic siltstones (**Figure 2**).

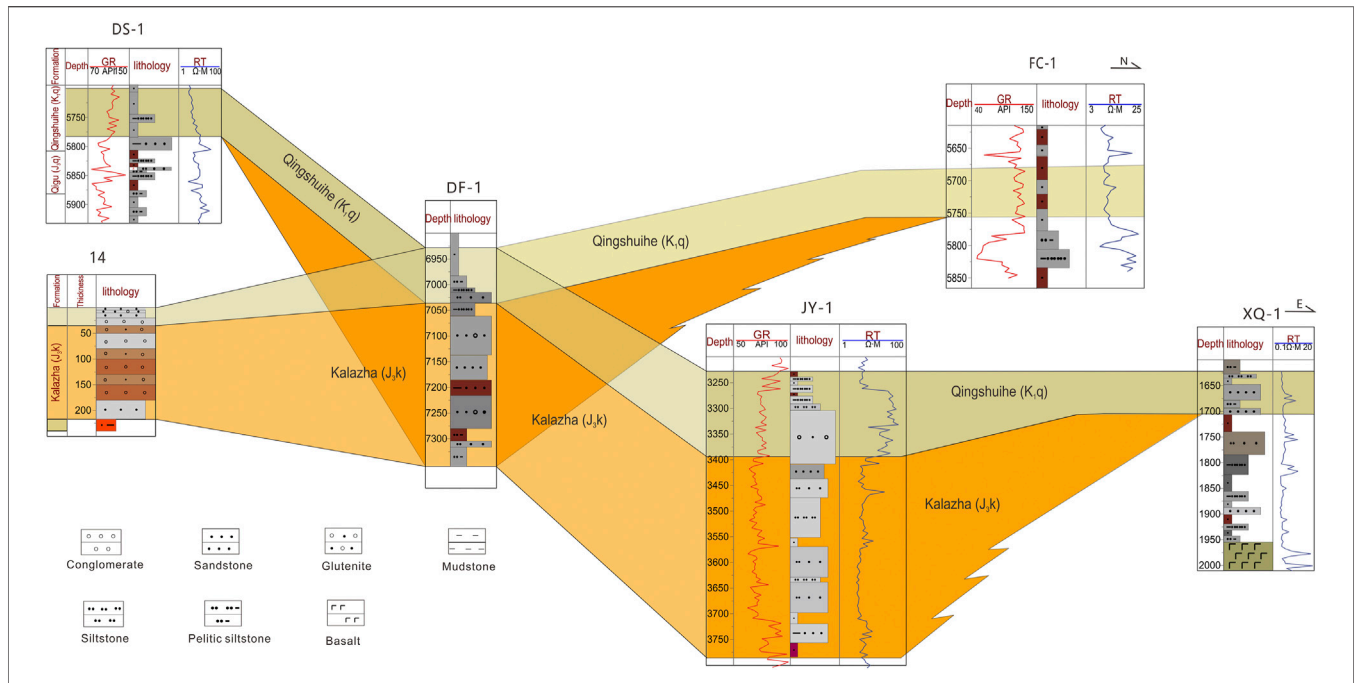


FIGURE 2 | Fence diagram showing cross-well stratigraphic correlation of the Kalazha Formation in the SMJB (location in **Figure 1**).

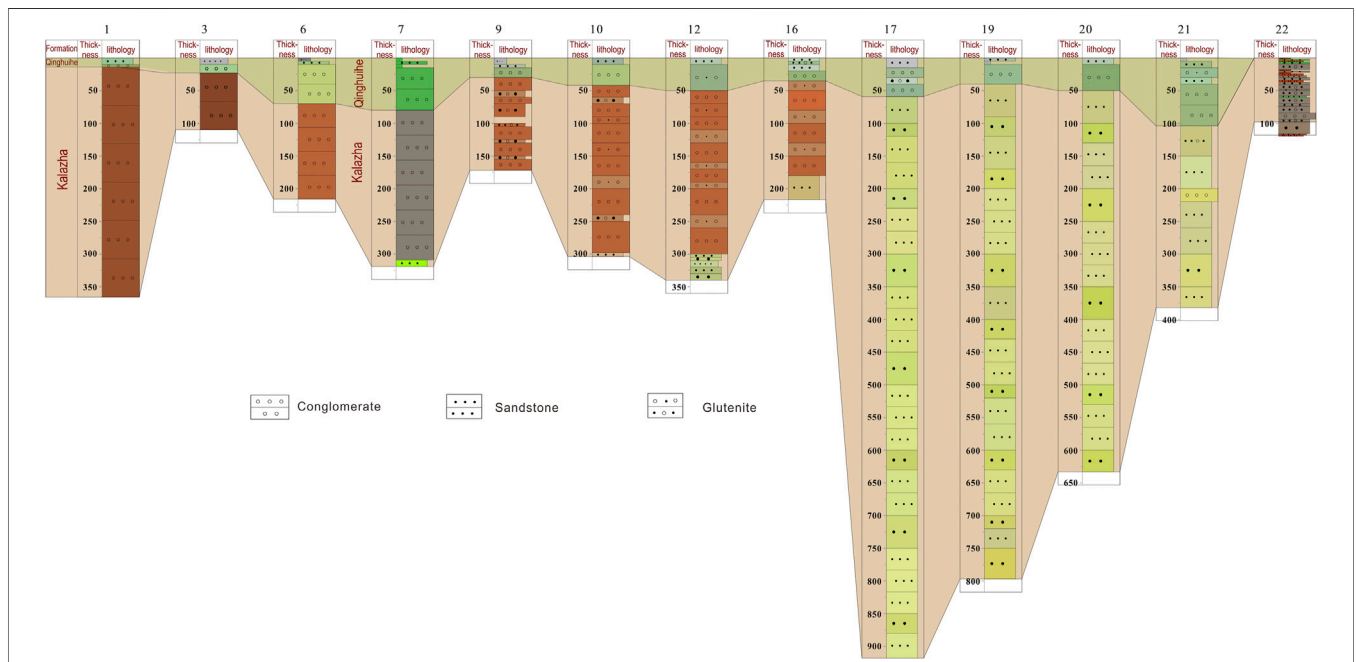
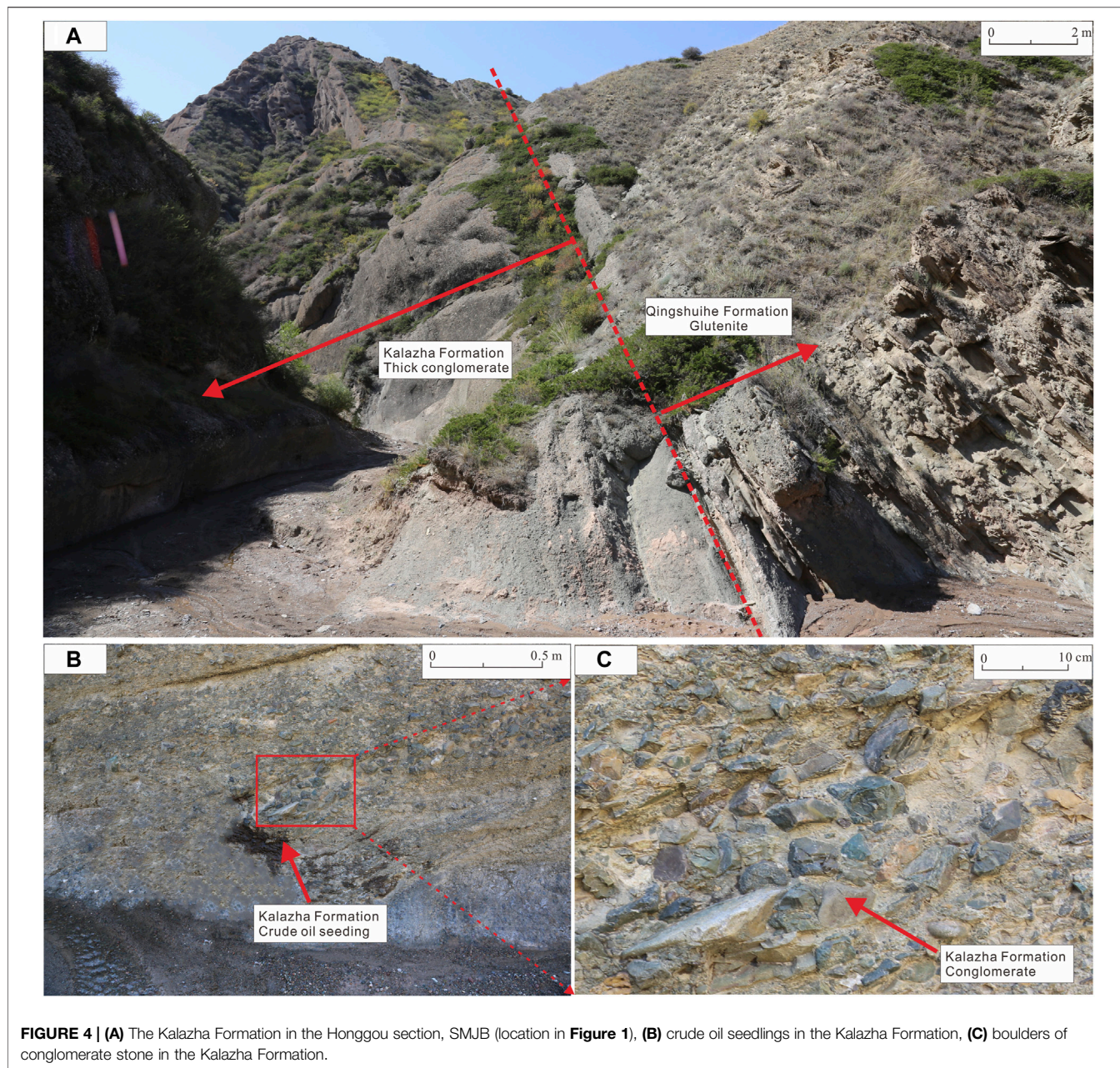


FIGURE 3 | Outcrop stratigraphic correlation of the Kalazha Formation in the SMJB (location in **Figure 1**).

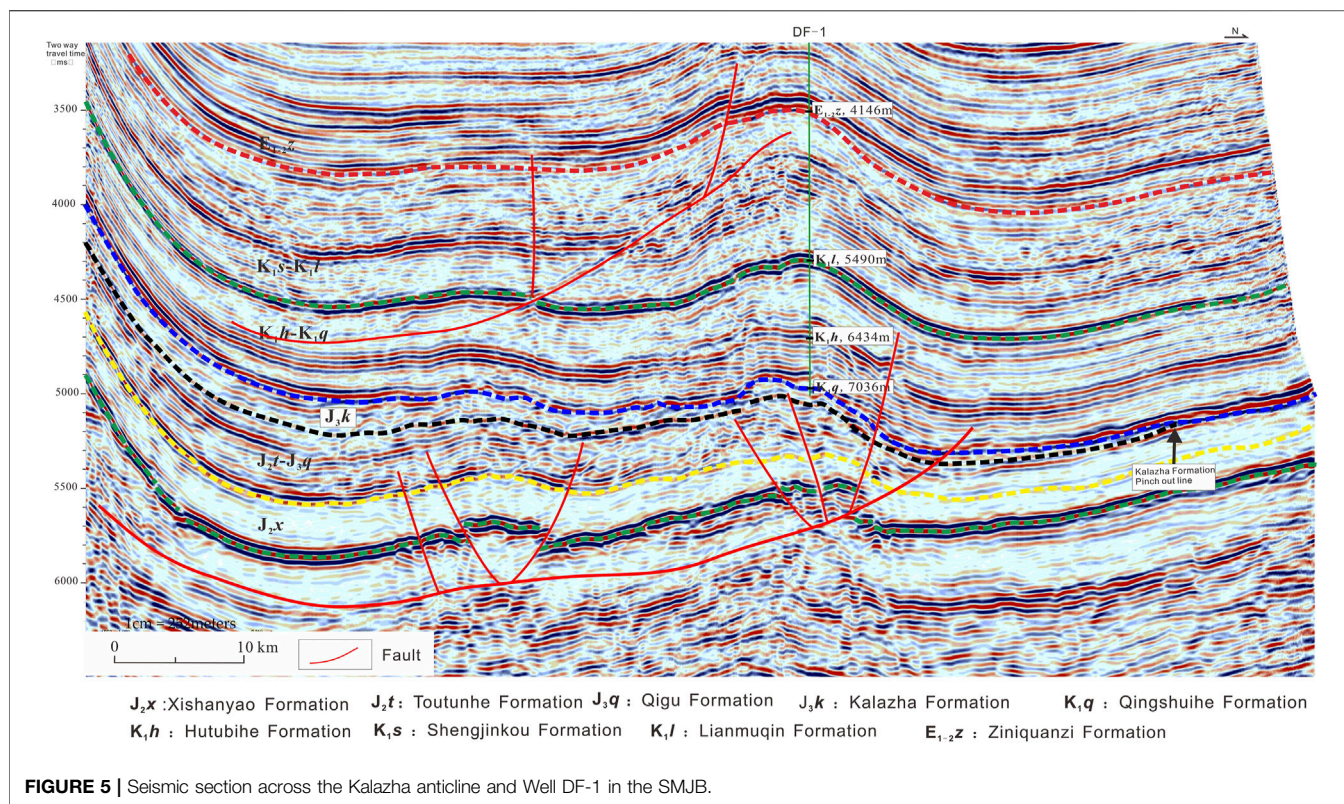
The Kalazha Formation at Well JY-1 is 390 m thick and mainly composed of medium-to-fine-grained sandstones and some conglomerates. As per the east-west and north-south cross-well stratigraphic correlation sections (**Figure 2**), the Kalazha Formation pinches out to the east of Well JY-1 and the west of

Well XQ1 in the east, between Wells DF-1 and DS-1 in the west, and the south of Well FC-1 in the north. According to outcrop observation, the Kalazha Formation lithologically consists of conglomerates and sandy conglomerates in the southern piedmont area and finestones and siltstones toward the north.



To further investigate the stratigraphic distribution and reservoir properties in the Kalazha Formation, we made a stratigraphic column based on the observation, measurement, and sampling of 22 outcrop sections in the area of interest (**Figure 1**) and performed stratigraphic correlation (**Figure 3**). The Kalazha Formation in the outcrop area is lithologically composed of thick, blocky brown, gray, and grayish green conglomerates; sandy conglomerates; and medium-to-coarse-grained sandstones (**Figure 4A**) 80–860 m thick. The largest thickness occurs in the Toutunhe section across the Kalazha anticline, where the Kalazha Formation is 860 m thick. Formation thickness decreases from east to west.

As per outcrop correlation, the Kalazha Formation consists of brown and gray conglomerates from the Ziniquanzi section in the west-east direction (no. 1 outcrop section) to the section across the south flank of the Aketun syncline between the Changji river and Toutunhe river (no. 16 outcrop section). Angular pebbles of various diameters occur chaotically with a low degree of roundness and high shale content (**Figures 4B,C**), which indicate near-source alluvial fan deposition (Shan et al., 2014; Guan et al., 2020). On the east of the section across the north flank of the Kalazha anticline in Toutunhe (no. 17 section), the Kalazha Formation consists of grayish green coarse sandstones and medium-to-fine-



grained sandstones with increased thickness (**Figure 3**), inferred to be braided river delta deposition (Si et al., 2018; Gao et al., 2020). In general, the Kalazha Formation in the area of interest is lithologically varied in the lateral direction. Conglomerates mainly occur in the southwestern piedmont area, especially west of Changji. Additionally, particle size decreases toward the north. Sandstones of braided river delta deposition turn up in the southeast, e.g., in Urumchi and Fukang, close to the Bogeda Mountain; this lithologically differs greatly from the sandy conglomerates of alluvial fan deposition in the southwest.

Using 2D and 3D seismic data and well-tie calibration, we located the Kalazha Formation in seismic sections and performed horizon interpretation based on seismic facies and cross-well stratigraphic correlation. The Kalazha Formation features weak reflections inside the region and chaotic reflections in the piedmont area (**Figure 5**), related to thick less-layered blocky sandy conglomerates. The lateral continuity of seismic reflections increases from the piedmont area to the north. As shown in several framework sections, the Kalazha Formation mainly extends in Manas, the Qigu faulted fold belt, Hutubi, and Fukang with topographically high areas in the north and low areas in the south. The Kalazha Formation wedges out in the updip direction from the piedmont area to the north (**Figure 5**) and was denuded at the east and west sides.

The Kalazha Formation is thick, laterally stable, and continuous. With respect to tectonic features, the structurally high piedmont thrust belt in the south changes into the

structurally low piedmont depressed zone, with a large, buried depth and slope zone and small, buried depth in the north. The formations incline in a monoclinical geometry toward the south with a small, buried depth in the south.

RESERVOIR PROPERTIES AND PREDICTION

We measured reservoir porosity and permeability using Kalazha core and outcrop samples acquired from the area of interest, including eight sandstone samples from Well CS-1 and more than 20 sandy conglomerate and sandstone samples from outcrops. As per cast thin sections from the Toutunhe section (no. 17 outcrop section) and Well CS-1, Kalazha sandstones have suitable reservoir properties with abundant highly interconnected pores, mainly intergranular pores and adequate particle sorting and roundness (**Figures 6A,B**). Kalazha conglomerates are of relatively poor reservoir properties. Cast thin sections of conglomerates from the Qingshuihe section (no. four outcrop section) showed a limited number of intergranular pores (**Figure 6C**) with poor connectivity and poor pebble sorting and roundness. Siltstones and finestones with small particle sizes turn up toward the lake basin in the north (**Figures 6D,E**). These deeply buried sandstones are tight in spite of the high sorting degree. For siltstone and finestone core samples acquired from Well HS1, the average porosity was tested to be 5.6%, and the average permeability was tested to be $0.028 \times 10^{-3} \mu\text{m}^2$. Kalazha sandstones are generally superior to

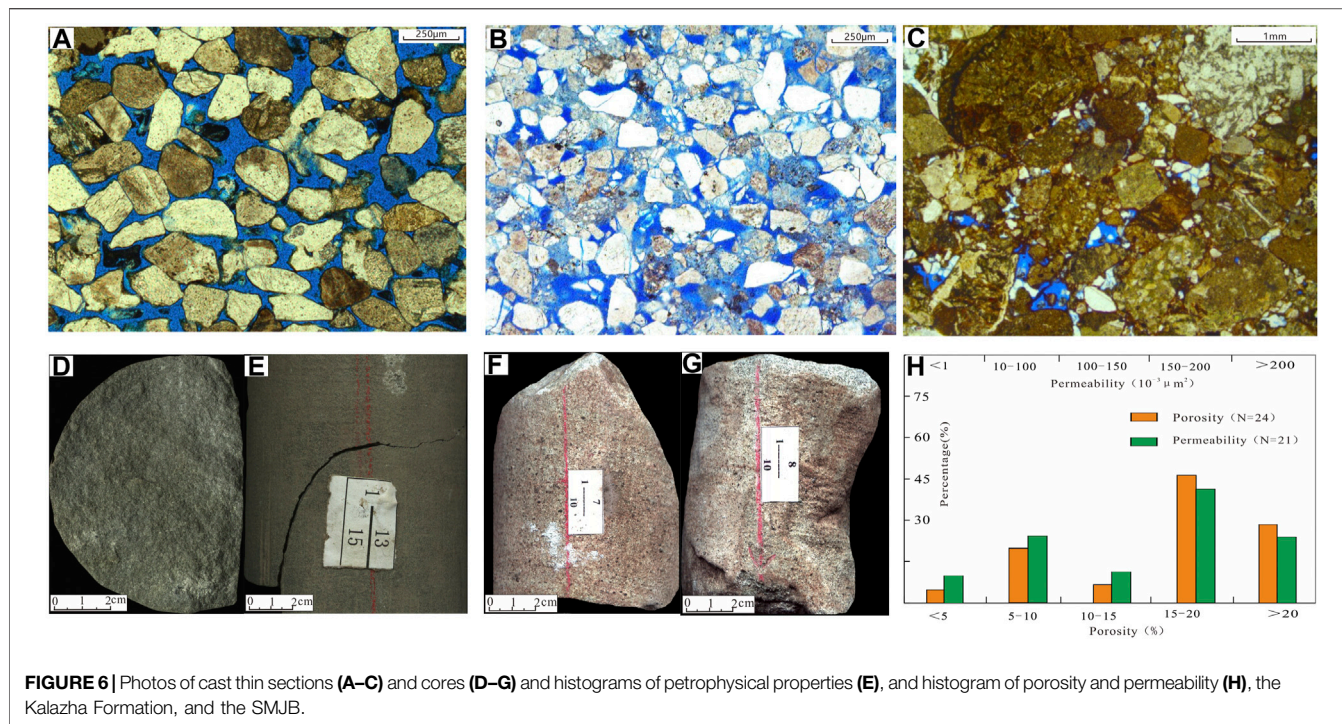


FIGURE 6 | Photos of cast thin sections (A–C) and cores (D–G) and histograms of petrophysical properties (E), and histogram of porosity and permeability (H), the Kalazha Formation, and the SMJB.

TABLE 1 | Impedance variation with lithology and buried depth in the SMJB.

Depth (m)	Impedance ($\text{g}/\text{cm}^3 \times \text{m}/\text{s}$)		
	Sandstone	Mudstone	Sandy conglomerate
<2,000	6,500–9,000	9,000–11,000	>11,000
2,000–4,500	7,500–10,000	10,000–12,000	>12,000
>4,500	9,000–12,000	12,000–13,000	>13,000

conglomerates in reservoir properties. Kalazha reservoir rocks in the Toutunhe section and Well CS-1 are mainly thick, medium-to-coarse-grained sandstones with massive bedding (Figures 6F,G). The porosity ranges from 5.7% to 25.7% with an average of 17.69%. The samples with the porosity above 15% account for 72% of the total samples. The permeability ranges from 0.8 to $260 \times 10^{-3} \mu\text{m}^2$ with an average of $175 \times 10^{-3} \mu\text{m}^2$. The samples with a permeability above $150 \times 10^{-3} \mu\text{m}^2$ account for 67% of the total samples (Figure 6H).

As per the correlation between lithology and impedance for the Kalazha Formation and Middle and Upper Jurassic Series at Wells JY-1, JY-2, CS-1, and XH-1, impedance generally increases with buried depth (Li et al., 2002). Within a specific depth range, the impedance varies with the lithologic association. Sandy conglomerates exhibit the largest impedance, followed by mudstones; sandstones exhibit the smallest impedance. Given the change in buried depth and impedance, the Kalazha Formation was divided into three intervals (above 2,000 m, between 2,000 and 4,500 m, and below 4,500 m) for the study of lithology–impedance relation.

At the interval shallower than 2,000 m, the data of Well CS-1 show sandstone impedance of $6,500\text{--}9,000 \text{ g}/\text{cm}^3 \times \text{m}/\text{s}$,

mudstone impedance of $9,000\text{--}11,000 \text{ g}/\text{cm}^3 \times \text{m}/\text{s}$, and sandy conglomerate impedance over $11,000 \text{ g}/\text{cm}^3 \times \text{m}/\text{s}$ (Table 1). At the interval of 2,000–4,500 m, the data of Wells JY-1 and JY-2 show sandstone impedance of $7,500\text{--}10,000 \text{ g}/\text{cm}^3 \times \text{m}/\text{s}$, mudstone impedance of $10,000\text{--}12,000 \text{ g}/\text{cm}^3 \times \text{m}/\text{s}$, and sandy conglomerate impedance over $12,000 \text{ g}/\text{cm}^3 \times \text{m}/\text{s}$. At the interval deeper than 4,500 m, the Kalazha Formation was drilled by only one well, i.e., DF-1. No deep-zone well logging was performed due to engineering issues, and thus, log data are unavailable. We used the data of Well XH1 drilled in a neighboring area, showing sandstone impedance of $9,000\text{--}12,000 \text{ g}/\text{cm}^3 \times \text{m}/\text{s}$, mudstone impedance of $12,000\text{--}13,000 \text{ g}/\text{cm}^3 \times \text{m}/\text{s}$, and sandy conglomerate impedance over $13,000 \text{ g}/\text{cm}^3 \times \text{m}/\text{s}$.

1) Toutunhe section, Kalazha formation, medium sandstone; 2) Changshan 1,764.16 m, Kalazha formation, medium fine sandstone; 3) Qingshuihe section, Kalazha formation, glutenite (Si et al., 2020; internal communication); 4) Hutan 17,365.3 m, Kalazha formation, silty fine sandstone; 5) Hutan 17,366.45–7,366.5 m, Kalazha formation, siltstone; 6) Changshan 1,764.5–764.6 m, Kalazha formation, fine sandstone; 7) Changshan 1,764.6–764.7 m, Kalazha formation, fine sandstone; and 8) physical property histogram of sandstone reservoir of Kalazha formation.

According to the impedance variations with lithology and buried depth in the Kalazha Formation, we used 2D and 3D seismic data for impedance inversion and reservoir prediction. As per joint 2D and 3D inversion results, blocky Kalazha reservoirs are generally over 100 m thick and extend consistently in the lateral direction with suitable inter-connectivity. Formation thickness decreases from south to north and finally vanishes.

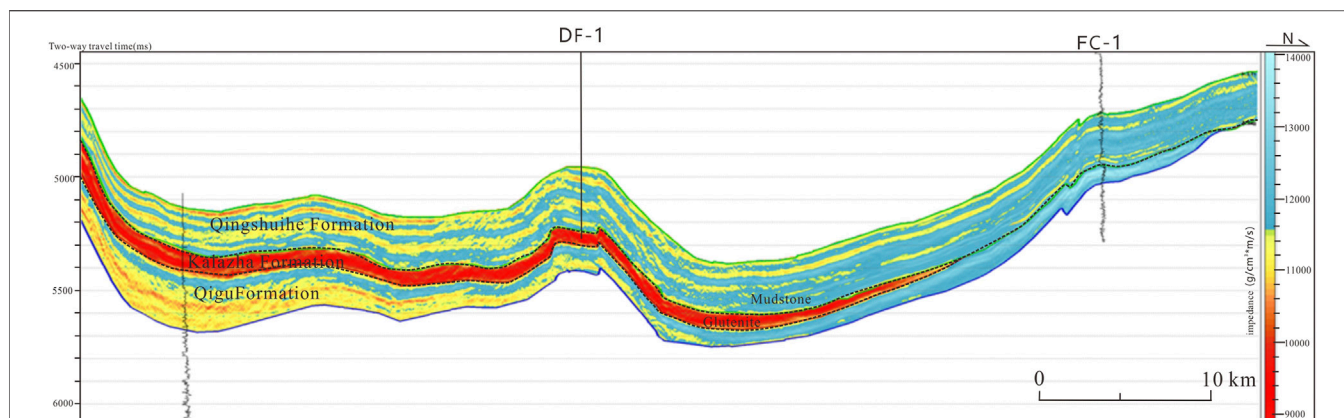


FIGURE 7 | Inverted impedance section across Wells DF-1 and FC-1 in the SMJB.

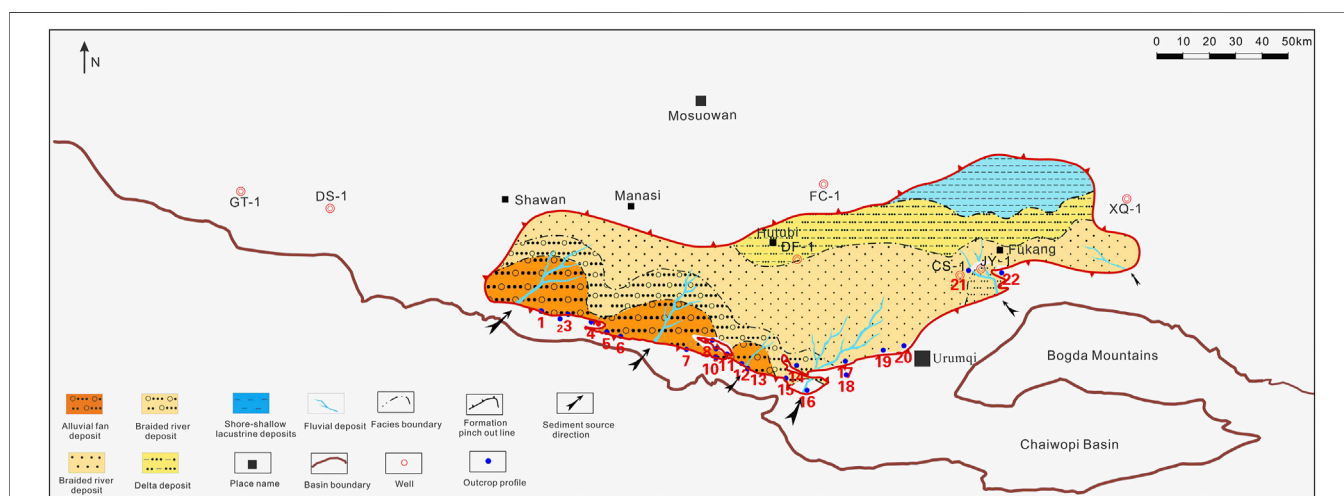


FIGURE 8 | Stratigraphic distribution of the Jurassic Kalazha Formation in the SMJB.

Reservoir rocks are overlain and underlain with mudstones (Figure 7). Sandstone reservoirs mainly occur in the northeast, e.g., Fukang on the north of the Bogeda Mountain. Sandy conglomerate reservoirs mainly occur in the southwest piedmont area, e.g., the Qigu faulted fold belt and Manas (Figure 8).

The study of Kalazha sedimentation was based on seismic inversion and reservoir prediction and well drilling and outcrop data. As per the sedimentation in the outcrop sections, the Kalazha Formation has different lithologic associations. On the west of the section across the south flank of the Aketun syncline between the Changji river and Toutunhe river (no. 16 outcrop section), the Kalazha Formation is composed of thick blocky brown or grayish brown conglomerates and sandy conglomerates of typical alluvial fan deposition with chaotically arranged pebbles, a low sorting degree, and high shale content, as mentioned above. A lake basin system occurs in the north with

enhanced water power and fine-grained sandstones and siltstones deposited (Figures 6D,E). In the outcrop area on the east of the section across the north flank of the Kalazha anticline in Toutunhe (no. 17 section), the Kalazha Formation is mainly composed of sandstones with basal scouring structure. Trough cross-bedding and massive bedding shown in the cores from Well CS-1 (Figures 6F,G) indicate underwater distributary channel deposition in the braided river deltaic front (Si et al., 2018). Sand particle size decreases toward the northwest. It is hard to delineate the alluvial fan system or the braided river deltaic system in the lake basin for lack of deep-well data. Thus, we inferred the intrafacies and their boundary (Figure 8), according to the depositional model and lithology-varied impedance. Detailed sedimentary microfacies will be classified using more well data.

As shown on the sedimentary system map, the Kalazha Formation in the southwest piedmont area is mainly composed of conglomerates (Figure 8) with large impedance,

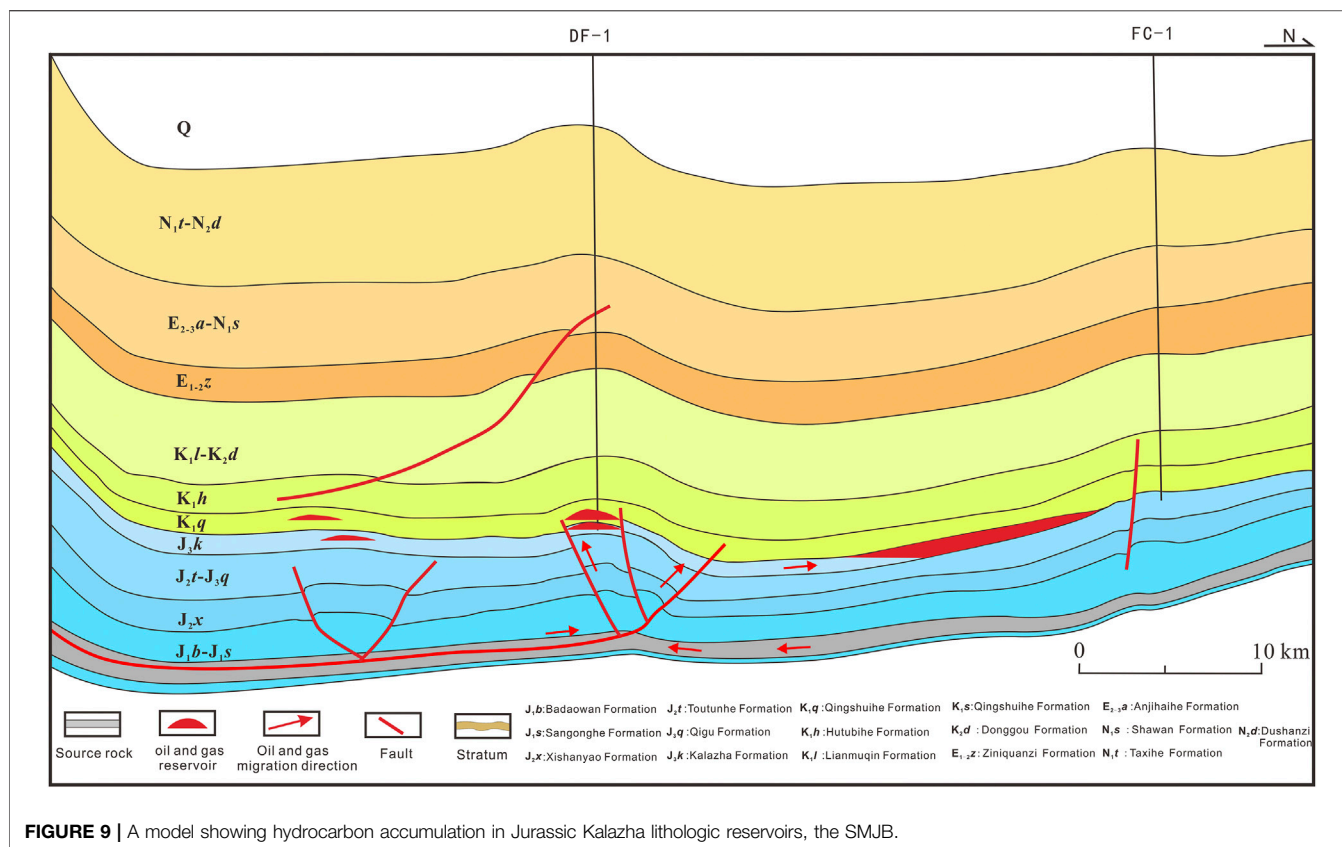


FIGURE 9 | A model showing hydrocarbon accumulation in Jurassic Kalazha lithologic reservoirs, the SMJB.

which change into medium-to-fine-grained sandstones and siltstones with small impedance in the north and vanish at last. Conglomerates seldom occur in the southeast. The formation is mainly composed of thick, layered sandstones of nearly 400 m thick with suitable reservoir properties, small impedance, and consistent lateral extension. High-graded reservoirs exhibit medium to low impedance. Shore-lake to shallow lacustrine argillaceous sediments were predicted to occur in the northeast.

ACCUMULATION MODEL AND PROMISING PROSPECTS

The Jurassic Kalazha Formation in the SMJB is among the most important exploration targets in the lower assemblage due to its promising hydrocarbon accumulation conditions. Kalazha reservoirs are underlain with several packages of deeply buried multi-type Middle and Lower Jurassic source rocks. The Lower Jurassic Badaowan Formation was deposited with dark mudstones 200–300 m thick, carbonaceous mudstones, and coals. Dark mudstones in the San'gonghe Formation are 50–300 m thick. Dark mudstones and carbonaceous mudstones in the Middle Jurassic Xishanyao Formation are 75–150 and 2–15 m thick, respectively. Crude oil originating from the Jurassic System in the Qigu and Kayindike oilfields (Wang et al., 2013; Chen et al., 2015) demonstrated wide

extension and credibility of Jurassic source rocks in the SMJB. Mature to post-mature source rocks may generate sufficient oil and gas for overlying reservoirs. Thus, the Kalazha Formation is rich in oil and gas resources.

Kalazha sandstone and sandy conglomerate reservoirs feature large thickness and suitable properties, favorable for hydrocarbon accumulation. The overlying regional capping bed in the Cretaceous Tugulu Group extends consistently in the lateral direction, where high to extremely high formation pressure enhances the sealing performance of mudstone overburden for the preservation of Kalazha oil and gas reservoirs. As shown in the Honggou outcrop section (Figure 8), oil seepage with large viscosity could be observed frequently in the Kalazha Formation (Figure 4), which evidences the promising accumulation conditions in the Kalazha Formation in the area of interest.

We established an accumulation model for Jurassic Kalazha lithologic reservoirs in the SMJB, according to the source rocks, reservoir rocks, caprocks, and migration system (Figure 9). Source conditions are promising in view of mature to highly mature coal-measure source rocks in the Middle and Lower Jurassic System. Downward detachment faults and associated secondary faults inside Lower Jurassic coal measures strata and unconformable surfaces constitute an effective migration system. Due to a high degree of plasticity in coal measures strata, detachment and deformation tend to occur in the process of compressional

overthrusting to form fractures. Detachment faults and associated faults constitute a vertical migration system in the Kalazha Formation (Figures 5, 9). The Jurassic Kalazha Formation lies unconformably below the Cretaceous Qingshuihe Formation. Thick sandy conglomerates at the bottom of the Qingshuihe Formation extend consistently in the lateral direction and could function as the lateral carrier bed (Kuang and Jia, 2005; Li et al., 2006).

Sediments from the south sedimentary source in the Kalazha Formation were unloaded and accumulated in the fore-deep sags in the thrust belt to form thick sands, which wedge out in the updip direction toward the north. Thus, the slope zone in the thrust belt is geologically favorable for lithologic traps.

In conclusion, the Kalazha Formation has favorable hydrocarbon accumulation conditions. Mass oil and gas generated by Middle and Lower Jurassic source rocks may migrate into reservoir rocks along microcracks in the source rocks and into shallow zones and structural highs along the system composed of detachment faults. Oil and gas may migrate laterally along continuous inter-connected sands in the Kalazha Formation. Owing to the effect of buoyancy force, oil and gas will flow toward the shallow zones in the north along laterally connected sands in the Kalazha Formation and accumulate in those lithologic traps with top mudstone overburden to form lithologic hydrocarbon reservoirs.

According to the accumulation model and stratigraphic and structural features of the Kalazha Formation, the promising prospects were anticipated to be lithologic traps in the annular zone, wedging out in the updip direction of the north slope, which has been the destination of hydrocarbon migration in a long period and is covered with thick mudstones in the updip direction. Lithologic reservoirs may concentrate in this zone. The area with the Kalazha Formation is also important for gas exploration in view of highly to post-mature Jurassic source rocks for gas generation in deep zones. We should make full use of 2D and 3D seismic data to perform lithologic trap identification and prediction and offer support to gas exploration.

CONCLUSION

The following conclusions can be drawn:

- 1) The stratigraphic distribution and features of the Jurassic Kalazha Formation were revealed in the SMJB based on individual-well analysis, cross-well stratigraphic correlation, well-tie calibration, and seismic reflections. Due to intense denudation, the Kalazha Formation is limited within Manas, Hutubi, Fukang, and Qigu faulted fold belt in the SMJB. It pinches out from the piedmont area to the north in the updip direction and was denuded in the east and west. The formation exhibits a monoclinical geometry with structurally high areas in the north and structurally low areas in the south.
- 2) The relations were established between impedance and different lithologies, i.e., sandstone, mudstone, and sandy conglomerate, at different depths in the Kalazha Formation

based on individual-well lithology–impedance correlation. Reservoir distribution in the Kalazha Formation was predicted using joint 2D and 3D seismic impedance inversion, showing major Kalazha reservoir rocks, i.e., sandy conglomerates and sandstones, 100–400 m thick. According to seismic inversion and outcrop sections, the Kalazha Formation in the southwest was diagnosed as a fan deltaic deposition with sandy conglomerate reservoirs close to the piedmont source area and fine-grained reservoir rocks in the north. The Kalazha Formation in the southeast was diagnosed as a braided river deltaic deposition with sandstone reservoirs of suitable petrophysical properties.

- 3) According to the study of source rocks, reservoir rocks, caprocks, and migration system, the Kalazha Formation in the SMJB was geologically favorable for large-scale hydrocarbon accumulation in lithologic reservoirs, establishing an accumulation model for lithologic reservoirs. Based on the accumulation model, the promising prospects were predicted to be lithologic traps in the annular wedge-out zone in the north foreland slope. Efforts should focus on lithologic trap identification and prediction in this region.

DATA AVAILABILITY STATEMENT

The raw data supporting the conclusion of this article will be made available by the authors, without undue reservation.

AUTHOR CONTRIBUTIONS

GL (first author and corresponding author) made significant contributions in the writing—original draft and manuscript revision, research ideas, sample collection, experimental analysis, and data analysis. J-ZL put forward and improve the research process and ideas. X-FQ made significant contributions in the reservoir-forming process simulation. MZ helped with sample collection. BY made significant contributions in the reservoir sample collection and data analysis. Z-CP made significant contributions in drawing the figures and data analysis. All authors contributed to the article and approved the submitted version.

FUNDING

This study was supported by the advanced research fund project of CNPC (No. 2019D-500801) and the Major Science and Technology project of CNPC (No. kt2020-0404).

ACKNOWLEDGMENTS

We are particularly grateful to the editorial department and the reviewers for their patience and hard work.

REFERENCES

- Chen, J. P., Wang, X. L., Deng, C. P., Zhao, Z., Ni, Y. Y., Sun, Y. G., et al. (2015). Geochemical Features of Source Rocks in the Southern Margin, Junggar Basin, Northwest China. *Acta Petrol. Sin.* 36 (7), 767–780. doi:10.7623/syxb201507001
- Chen, J., Deng, C., Wang, X., Ni, Y., Sun, Y., Zhao, Z., et al. (2017). Formation Mechanism of Condensates, Waxy and Heavy Oils in the Southern Margin of Junggar Basin, NW China. *Sci. China Earth Sci.* 60, 972–991. doi:10.1007/s11430-016-9027-3
- Chen, J. P., Wang, X. L., Ni, Y. Y., Xiang, B. L., Liao, F. R., Liao, J. D., et al. (2019). Genetic Type and Source of Natural Gas in the Southern Margin of Junggar Basin, NW China. *Pet. Explor. Develop.* 46, 461–472. doi:10.1016/S1876-3804(19)60029-7
- Darby, D., Stuart Haszeldine, R., and Couples, G. D. (1996). Pressure Cells and Pressure Seals in the UK Central Graben. *Mar. Pet. Geol.* 13 (8), 865–878. doi:10.1016/S0264-8172(96)00023-2
- Du, J. H., Zhi, D. M., Li, J. Z., Yang, D. S., Tang, Y., Qi, X. F., et al. (2019). Major Breakthrough of Well Gaotan 1 and Exploration Prospects of Lower Assemblage in Southern Margin of Junggar Basin, NW China. *Pet. Explor. Develop.* 46 (02), 15–25. doi:10.1016/S1876-3804(19)60003-0
- Fu, X., Du, X. F., Guan, D. Y., Wang, Q. M., and Ye, M. S. (2020). Depositional System, Plane Distribution and Exploration Significance of Fan-Delta Mixed Siliciclastic-Carbonate Sediments in Lacustrine Basin: An Example of Member1-2 of Shahejie Formation in Offshore Bohai Bay, Eastern China. *Earth Sci.* 45 (10), 3706–3720. doi:10.3799/dqkx.2020.173
- Gao, Z. Y., Feng, J. R., Cui, J. G., Zhou, C. M., and Shi, Y. X. (2020). Comparative Analysis on Sedimentary and Reservoir Characteristics of Jurassic to Cretaceous between Foreland Basins in Southern and Northern Tianshan Mountains. *Xin Jiang Pet. Geol.* 41 (1), 80–90. doi:10.7657/XJPG20200110
- Guan, X. T., Wu, C. D., Wu, J., Zhou, J. Q., Jiao, Y., Zhou, R., et al. (2020). Sedimentary Sequence and Sedimentary Environment Evolution of Upper Jurassic and Lower Cretaceous in the Southern Margin of Junggar Basin. *Xinjiang Pet. Geol.* 041 (001), 67–79. doi:10.7657/XJPG20200109
- He, D. F., Zhang, L., Wu, S. T., Li, D., and Zhen, Y. (2018). Tectonic Evolution Stages and Features of the Junggar Basin. *Oil Gas Geol.* 39 (05), 5–21. doi:10.11743/ogg20180501
- Jia, C. Z., Zhao, W. Z., Zou, C. N., Feng, Z. Q., Yuan, X. J., Chi, Y. L., et al. (2007). Geological Theory and Exploration Technology for Lithostratigraphic Hydrocarbon Reservoirs. *Pet. Explor. Develop.* 34 (3), 257–272. Available at <http://www.cpedm.com/CN/article/openArticlePDF.jsp?id=1474>.
- Jia, C. Z., Zhao, W. Z., and Zou, C. N. (2008). *Lithologic Stratigraphic Reservoir Geology Theory and Exploration Technique*. Beijing: Petroleum Industry Press, 162–180.
- Kuang, J., and Jia, X. Y. (2005). Relationship between Himalayan Movement and Hydrocarbon Accumulation in Southern Margin of Junggar Basin. *Xinjiang Pet. Geol.* 26 (02), 17–21. doi:10.3969/j.issn.1001-3873.2005.02.003
- Kuang, J., and Qi, X. F. (2006). The Structural Characteristics and Oil-Gas Explorative Direction in Junggar Foreland Basin. *Xinjiang Pet. Geol.* 27 (1), 5–9. doi:10.3969/j.issn.1001-3873.2006.01.002
- Kuang, L. C., Wang, X. L., Zhang, J., and Xia, H. P. (2012). Structural Modeling of the Huoerguoshi-Manashi-Tugulu Thrust belt at the Southern Margin of the Junggar Basin and the Discovery of the Mahe Gas Field. *Nat. Gas Industry* 32 (2), 11–15. doi:10.3787/j.issn.1000-0976.2012.02.003
- Lei, D. W., Chen, N. G., Li, X. Y., and Zhang, Y. C. (2012). The Major Reservoirs and Distribution of Lower Combination in Southern Margin of Junggar Basin. *Xinjiang Pet. Geol.* 33 (6), 648–650. Available at <http://www.zxjjpg.com/CN/abstract/abstract1132.shtml>.
- Li, L. C., Wu, J., Zhang, S., Zhuang, X. J., Zou, Y. P., and Wang, W. Z. (2002). Application of Seismic Wave Resistance Inversion in Sequence Stratigraphy Research—An Example of Junggar Basin. *Xinjiang Pet. Geol.* 23 (03), 70–81. doi:10.3969/j.issn.1001-3873.2002.03.020
- Li, X. Y., Shao, Y., and Li, T. M. (2003). Three Oil-Reservoir Combinations in South Marginal of Junggar Basin, Northwest China. *Pet. Explor. Develop.* 30 (6), 32–34. doi:10.3321/j.issn:1000-0747.2003.06.009
- Li, X. Y., Wang, B., and Chen, Y. (2006). The Fracture Patterns and Oil-Controlled Process in Piedmont on the Bruchfallen Zone Southern Margin of Junggar Basin. *Xinjiang Pet. Geol.* 27 (3), 285–287. doi:10.3969/j.issn.1001-3873.2006.03.006
- Liang, W., and Li, X. P. (2020). Lithological Exploration and Potential in Mixed Siliciclastic-Carbonate Depositional Area of Eastern Pearl River Mouth Basin. *Earth Sci.* 45 (10), 3870–3884. doi:10.3799/dqkx.2020.174
- Liu, G., Wei, Y. Z., Luo, H. C., Chen, G., Gong, D. Y., Wang, F., et al. (2018). Sand-body Structure and Reservoir Forming Control of Jurassic Sangonghe Formation in Well Block Shinan 13, Luxi Area, Junggar Basin. *Acta Petrol. Sin.* 39 (9), 1006–1018. doi:10.7623/syxb201809005
- Liu, G., Wei, Y. Z., Chen, G., Jia, K. F., Gong, D. Y., Wang, F., et al. (2019). Forming Mechanism, Distribution Characteristics of Jurassic-Cretaceous Secondary Reservoirs in the central Junggar Basin. *Acta Petrol. Sin.* 40 (8), 914–927. doi:10.7623/syxb201908003
- Magara, K. (1993). Pressure Sealing: An Important Agent for Hydrocarbon Entrapment. *J. Pet. Sci. Eng.* 9 (1), 67–80. doi:10.1016/0920-4105(93)90029-E
- Nansheng, Q., Zhihuan, Z., and Ershe, X. (2008). Geothermal Regime and Jurassic Source Rock Maturity of the Junggar basin, Northwest China. *J. Asian Earth Sci.* 31, 464–478. doi:10.1016/j.jseae.2007.08.001
- Schneider, W., Zhao, X. F., Long, N. L., Zhao, Y. S., and Long, N. L. (1992). Sedimentary Environment and Tectonic Implication of Jurassic in Toutunhe Area, Junggar Basin. *Xinjiang Geol.* 10 (3), 191–201.
- Shan, X., Yu, X. H., Li, S. L., Li, S. L., Li, W., and Wang, Z. X. (2014). The Depositional Characteristics and Model of Kalazha Formation in Shuimogou profile, Junggar basin. *J. China Univ. Mining Techn.* 43 (2), 262–270. doi:10.13247/j.cnki.jcumt.2014.02.005
- Si, X. Q., Yuan, B., Guo, H. J., Xu, Y., and Chen, N. G. (2020). Bloomberg Reservoir Characteristics and Main Controlling Factors of Qingshuihe Formation in the Southern Margin of Junggar Basin. *Oil and Gas Geology* 41 (01), 38–45. doi:10.7657/XJPG20200106
- Si, X. Q., Shen, J. L., Chen, N. G., Xu, Y., Guo, H. J., and Yuan, B. (2018). “Sedimentary Characteristics and Model of Jurassic Kalazha Formation in Southern Margin of Junggar Basin,” in Abstracts of the 15th National Conference on Palaeogeography and Sedimentology, Chengdu, China, 2018 (Petroleum geology Committee of Chinese Petroleum Society)
- Tao, S. Z., Yuan, X. J., Hou, L. H., Zhang, G. S., Yang, F., Tao, X. W., et al. (2017). The Regularities of Formation and Distribution of Giant Litho-Stratigraphic Oil and Gas Field. *Nat. Gas Geosci.* 28 (11), 1613–1624. doi:10.11764/j.issn.1672-1926.2017.10.002
- Tian, X. R., Zhuo, Q. G., Zhang, J., Hu, H. W., and Guo, Z. J. (2017). Sealing Capacity of the Tugulu Group and its Significance for Hydrocarbon Accumulation in the Lower Play in the Southern Junggar Basin, Northwest China. *Oil Gas Geol.* 38 (2), 334–344. doi:10.11743/ogg20170213
- Tigert, V., and Al-Shaieb, Z. (1990). Pressure Seals: their Diagenetic Banding Patterns. *Earth Sci. Rev.* 29 (1), 227–240. doi:10.1016/0012-8252(90)90039-x
- Wan, L. G., Liu, D. M., and Hou, L. G. (2005). Structural Characteristics of Foreland Thrust belt in the Southern Junggar Basin. *Pet. Geophys. Explor.* 40 (b11), 40–45. doi:10.3321/j.issn:1000-7210.2005.z1.008
- Wang, X. L., Zhi, D. M., and Wang, Y. T. (2013). *Source Rocks and Hydrocarbon Geochemistry in Junggar Basin*. Beijing: Petroleum Industry Press, 1–565.
- Wei, D. T., Jia, D., Zhao, Y. C., Yang, H. B., Chen, T., Wu, L. Y., et al. (2007). Geochemical Characteristics of Crude Oil in the Southern Margin of Junggar Basin. *Oil and Gas Geology* 2007 (03), 433–440. 0253-9985(2007)03-0433-08
- Wei, D. T., Zhao, Y. C., Abuli, M. T., Chen, T., Yang, H. B., Wu, L. Y., et al. (2010). Difference of Hydrocarbon Accumulation in the Foreland Thrust-fold Belt of the Southern Junggar Basin. *Geol. J. China Univ.* 16 (3), 339–350. doi:10.3969/j.issn.1006-7493.2010.03.007
- Wu, J. H., Xiang, S. Z., Wu, X. Z., Chen, W., and Wu, J. (2002). Structures in East Part of Southern Margin in Junggar Basin and Their Formation Mechanism. *Xinjiang Pet. Geol.* 23 (3), 208–210. doi:10.3969/j.issn.1001-3873.2002.03.009
- Wu, K. Y., Zha, M., Wang, X. L., Qu, J. X., and Chen, X. (2005). Further Researches on the Tectonic Evolution and Dynamic Setting of the Junggar Basin. *Acta Geosci. Sin.* 26 (3), 217–222. doi:10.3975/cagsb.2005.03.04
- Xiao, L. X., Chen, N. G., Zhang, J., Shen, J. L., and Zhang, S. C. (2011). Sedimentary Systems of Paleogene Ziniquanzi Formation, South Edge of Junggar Basin. *Nat. Gas Geosci.* 22 (03), 58–63. doi:10.3969/j.issn.1674-151x.2015.19.020
- Yuan, X. J., Xue, L. Q., Chi, Y. L., Chen, Z. M., and Qu, Y. H. (2003). Sequence Stratigraphic and Subtle-Trap Characteristics of Lacustrine Depression

- basin. *Acta Pet. Sin.* 24 (3), 11–15. doi:10.3321/j.issn:0253-2697.2003.03.003
- Zhang, Y. J., and Liu, G. D. (2002). Characteristics and Evolution of Composite Petroleum Systems and the Exploration Strategy in Junggar basin, Northwest China. *Pet. Explor. Develop.* 29 (1), 36–39. doi:10.3321/j.issn:1000-0747.2002.01.009
- Zhen, M., Li, J. Z., Wu, X. Z., Wang, S. J., Guo, Q. L., Chen, X. M., et al. (2019). Potential of Oil and Natural Gas Resources of Main Hydrocarbon-Bearing Basins and Key Exploration Fields in China. *Earth Sci.* 44 (03), 833–847. doi:10.3799/dqkx.2019.957

Conflict of Interest: Authors GL, J-ZL, X-FQ are employed by China National Petroleum Corporation, and in the PetroChina Research Institute of Petroleum Exploration and Development. Authors MZ, BY, and Z-CP are employed by China National Petroleum Corporation, and in the Research Institute of Petroleum Exploration and Development, Xinjiang Oilfield.

The authors declare that the research was conducted in the absence of any commercial or financial relationships that could be construed as a potential conflict of interest.

Publisher's Note: All claims expressed in this article are solely those of the authors and do not necessarily represent those of their affiliated organizations, or those of the publisher, the editors and the reviewers. Any product that may be evaluated in this article, or claim that may be made by its manufacturer, is not guaranteed or endorsed by the publisher.

Copyright © 2022 Liu, Qi, Li, Zhu, Yuan and Pang. This is an open-access article distributed under the terms of the Creative Commons Attribution License (CC BY). The use, distribution or reproduction in other forums is permitted, provided the original author(s) and the copyright owner(s) are credited and that the original publication in this journal is cited, in accordance with accepted academic practice. No use, distribution or reproduction is permitted which does not comply with these terms.